Defence Science Journal, Vol. 75, No. 3, May 2025, pp. 285-292, DOI : 10.14429/dsj.20915

Computational-Efficient Signal Processing Solution to Frequency Quadrupler Based High-Frequency Vector Signal Generator

Devashish Arora[$,*], Girish Chandra Tripathi[#] and Meenakshi Rawat[#]

[$]Qualcomm India Pvt Ltd., Noida – 201 304, India
[#]Department of ECE, IIT Roorkee, Roorkee – 247 667, India
[*]E-mail: devaaror@qti.qualcomm.com

ABSTRACT

Due to advancements in technological trends, interest in frequency multipliers is increasing in the research community. However, the linearization approach on frequency multipliers differs from that of power amplifiers and hence cannot be directly implementable for end-to-end high-frequency systems. This paper discusses recent computational approaches and proposes a model for improving performance metrics, especially the adjacent channel power ratio. This paper shows theoretical trends, mathematical approaches to current trends, and the proposed model. It then establishes the theory by experimental implementation and compares the proposition results to the models in the literature.

Keywords: Adjacent channel power ratio; Frequency multipliers; Microwave engineering; Principal component analysis; Memory polynomial

1. INTRODUCTION

In recent years, due to the advancement of technological needs, a fundamental shift for higher frequencies has been observed. From an implementation point of view, cost is an important driving factor. Hence, a trade-off between the accurate requirements and the equipment cost is always needed. Therefore, to have a balanced selection of resources for optimum and reasonable output from equipment(s), Frequency Multiplication (FM) is one area of vital interest for high-frequency communication, which is one of the key reasons that frequency multipliers are among the core components and areas of interest in literature. Hence, the literature contains extensive works on FMs in this field of area. This paper presented here is extended version of the paper presented in second international conference on microwave, antenna and communication[1].

Frequency multipliers are helpful in several conditions; for example, FM may be used to avoid a complete RF chain[2]. Thereby saving costs for the entire system. Another example where FMs may be of great importance is where the high frequencies are needed owing to the f_{max} limit of FMs > f_{max} limit of transistors[3]. In addition, FM helps translate the frequencies to produce steady envelope modulation[2]. FMs are highly nonlinear and tend to have distortions in AM modulations[2]. The distortions in FMs are not just in amplitude but also in phase. Hence, the envelope of the output would not be as desired[3]. This particular drawback gives the intent to have linearization of frequency multipliers, which is vital and would thereby impact the complete system. In literature, linearization, especially DPD of power amplifiers, has been widely covered[4–8]. In open texts, frequency quadrupling architectures have been proposed by authors using linearization with DPD and allowing the signal to have low distortion at the output[9]. Also, in literature, the frequency quadrupler transmitter's new arch was shown to have DPD linearization[9]. Authors investigated frequency quadruplers at 3.56 GHz as a proof of concept, wherein the QMP model was devised for forward modelling and based on it, the QDPD model was shown to be developed for inverse modelling of frequency multipliers for enablement of linearization[3].

However, using direct PA DPD implementation in FMs is not feasible mainly due to the following: 1) nth-order phase multiplication not being considered in the DPD linearization of PA[3], 2) DAC/ADC with high speed is required to implement DPD of PA in FMs[10], thereby increasing the cost of implementation of the entire system. Therefore, linearization of power amplifiers cannot be directly implemented in frequency multipliers. For FM specific in literature, feedback DPD in stages using cascaded methodology has been shown[10]. Also, the authors used GMP-nth-order power nonlinear models for FMs[10]. Also, in recent papers, DPD-based CFNN has been shown to offset distortions in frequency quadrupler, which was validated at 24 GHz and showed linearity restoration[11]. The authors demonstrated a new modified polynomial model computational approach for improvement of ACPR over state-of-art approaches of MP and GMP models for frequency quadruplers[1]. This paper attempts to extend it with wavelet decomposition and multiscale principal component analysis by enhancing in/out of band results, whose mathematical approach is covered in detail in the second section.

This paper has been organized into the following segments: mathematical computational system approaches

Received : 22 January 2025, Revised : 04 April 2025
Accepted : 29 April 2025, Online published : 08 May 2025

of state-of-the-art & current modelling have been covered in the second segment, also the mathematical modelling of the proposed system has been described in segment two. Segment three describes the physical realization of the experimental setup and implementation of the experiment for the modelling described in segment two. Further, in segment four, results are shown, and a comparison to the performance of state-of-the-art models and recent approaches is shown, followed by the fifth segment comprising conclusions.

2. SYSTEM MODELING AND COMPUTATIONAL APPROACHES

A number of models have been described in the literature[11-12] to overcome nonlinearities. Along with classical modelling approaches, new techniques and algorithms have been developed and are there, in theory, which set the foundations for experimental applications that can be used to enhance the newly proposed approaches, which will be depicted in the next section and thereby are physically realised in subsequent sections.

2.1 Polynomial-Based Models

To effectively tackle the memory-based nonlinearities shaped by prior inputs[1,12], it is imperative to investigate polynomial-based models. This section covers classical polynomial-based approaches, which are the foundations of computational approaches proposed in the subsequent sections.

2.1.1 Memory Polynomial Model

In literature, the Hammerstein model consists of a nonlinearity followed by a linear filter model (g)[12]. It can be generalized by employing different filters for each order k, organized in a two-dimensional array with power series coefficients b_{km}. For narrowband signals, combinations of the form $\beta(n)\,|\,\beta(n-m)\,|^{(k-1)}$ yield memory polynomial, which can be defined below[1,12] :

$$\gamma_{MP}(n)=\sum_{k=0}^{K-1}\sum_{m=0}^{M-1}b_{km}\beta(n-m)\,|\,\beta(n-m)\,|^{k} \tag{1}$$

where, k denotes the order of the envelope.

The Eqn. (1) illustrates that the output can be defined as a polynomial function of the present input signal alongside its previous values, thus embodying the system's nonlinear behaviour.

2.1.2 Generalized Memory Polynomial Model

The memory polynomial depicted in the previous section can be extended in a broader paradigm by introducing delays and time-domain offsets between the signal and envelope[1,11,12]. Thus, the generalized polynomial model can be characterized as follows:

$$\begin{aligned}\gamma_{GMP}(n)=&\sum_{k=0}^{K_a-1}\sum_{l=0}^{L_a-1}a_{kl}\beta(n-l)\,|\,\beta(n-l)\,|^{k}\\&+\sum_{k=1}^{K_b}\sum_{l=0}^{L_b-1}\sum_{m=1}^{M_b}b_{klm}\beta(n-l)\,|\,\beta(n-l-m)\,|^{k}\\&+\sum_{k=1}^{K_c}\sum_{l=0}^{L_c-1}\sum_{m=1}^{M_c}c_{klm}\beta(n-l)\,|\,\beta(n-l+m)\,|^{k}\end{aligned} \tag{2}$$

The number of coefficients for signal-strength, signal-retarded & signal-advanced envelope(s) are specified by K_aL_a, $K_bL_bM_b$ & $K_cL_cM_c$ respectively[1,3,11,13].

2.1.3 Q-MP Model (Frequency Quadrupler specific based Model)

For a frequency multiplier, the output can be represented as follows[3]:

$$\gamma(t)=\sum_{n=1}^{N}\alpha_n\beta^{n}(t) \tag{3}$$

here, α_n are coefficients & N is nonlinearity order.

Thus, for an input modulated signal $\beta(t)$ with magnitude $\lambda(t)$ and phase $\theta(t)$, the output equation of frequency multiplier will be as in following Eqn. (4)[1,3,11].

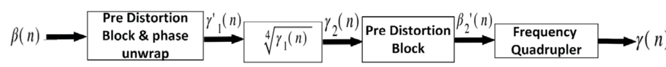

Figure 1. Standard Computational Approach 1: Dual Stage Approach[1,11,14,15].

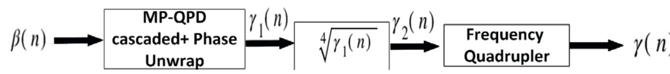

Figure 2. Standard Computational Approach[21,3,11].

$$\gamma(t)=\sum_{n=1}^{N}\alpha_n\ \lambda(t)\cos(\omega_c(t)+\theta(t))^{\ n} \tag{4}$$

Now, for the frequency quadrupler, only the harmonics of order four would be accounted for as follows[3]:

$$\gamma_{4\omega_c}(t)=\sum_{k=1}^{K}c_k\lambda^{4}(t)\cos(4\omega_c+4\theta(t))\lambda^{2(k-1)}(t) \tag{5}$$

The above is an RF passband form of frequency quadrupler without memory effects where K is nonlinearity order, c_k is coefficient of k^{th} order and $\lambda(t)$ is the magnitude of $\beta(t)$ signal[3]. The Eqn (5) shows that the frequency expansion & phase are changing in the order of four due to the frequency quadrupler being in action. However, Eqn. (5) also gives us the insight that even harmonics from higher-order nonlinearities, i.e., greater than four for a quadrupler also, affect the output[1,3]. In extension to the Eqn. (5), the equation can also be expressed in complex baseband form without memory effects by substituting $\beta(n)=\lambda(n)e^{j\theta(n)}$ leads to the following output[3]:

$$\gamma(n)=\sum_{k=1}^{K}c_k\beta^{4}(n)\,|\,\beta(n)\,|^{2(k-1)} \tag{6}$$

To incorporate memory effects, the above equation can be redefined, including the memory terms below[1,3]:

$$\begin{aligned}\gamma_{QMP}(n)=&\sum_{m_1=0}^{M_1-1}\sum_{m_2=0}^{M_2-1}\cdots\sum_{m_n=0}^{M_n-1}\sum_{k=1}^{K}c_{m_1m_2......m_nk}\cdot\cdot\\&\ldots\beta^{4}(n-m_1)\beta(n-m_2)\ldots|\,\beta(n-m_n)\,|^{k-1}\end{aligned} \tag{7}$$

In Eqn. (7), $M_1, M_2....M_n$ represent memory depth, k depicts the order of nonlinearity and $c_{m_1m_2......m_nk}$ represent the complex coefficients.

2.2 Computational Approaches for Frequency Quadrupler

In conventional approaches to power amplifiers, the forward model and inverse model are similar to each other;

therefore, forward-inverse models are swappable for an inverse input-output relationship; but, as observed in the previous section, due to the nth-order nature of the nth frequency multiplier (*n=4 for quadrupler*), the frequency multipliers cannot have direct inverse input-output relationship by swapping each-other[3]. Thus, direct implementation of conventional techniques used in power amplifiers is not possible. Thus, there is a need to have different approaches for frequency quadruplers, which are covered in this section.

2.2.1 Direct Computational Approach

In literature[1,3,11,14], to do inverse modelling, one method is to directly swap $\gamma(n)$ and $\beta^4(n)$ & thereby, extract the complex coefficients for the generation of the DPD signal; however, direct implementation gives rise to an abrupt shift in signal along with 2π phase change due to Gibb's phenomena leading to increase in noise which leads to decrement of NMSE (covered in subsequent section) and thus leads to signal quality degradation. Hence, as mentioned above, direct implementation is not recommended due to its drawbacks.

2.2.2 Standard Computational Approaches (SCA)

SCA1: In literature, as per papers[11,14,15] in Fig. 1, there is a dual-stage approach wherein the signal $\beta(n)$ is first passed through the Pre-Distortion block to provide output, which is then subsequently passed through the phase unwarp block to give $\gamma'(n)$ (to avoid Gibb's phenomena), which is then passed through the multiplicative root F, i.e., (1/4 for quadrupler) to provide $\sqrt[F]{\gamma_1'(n)}$.

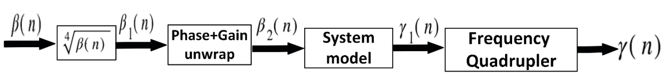

Figure 3. New modified polynomial model computational approach[1].

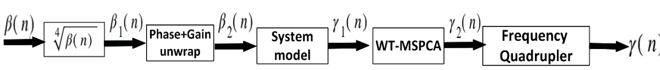

Figure 4. Proposed computational approach for frequency quadrupler.

This method uses a multiplicative root block to correct AM and PM distortions[11,14-15] to relax the linearity requirement for the next pre-distortion block, whose output is $\gamma_2(n)$[11]. After this, up-conversion can now be done. First conversion is done at intermediate frequency (f_{IF}) and then subsequently also upscaled by order of F(F=4 for quadrupler) & then filtered to have the final RF output signal $\gamma(n)$[1,11,15]

SCA2: This computational method is shown in Fig. 2, wherein the input signal $\beta(n)$ is passed through a cascade MP & QDPD (MP-QPD), leading to output as $\gamma_1(n)$[1,3,11] allowing linearization of frequency quadrupler to be done using QDPD and remaining distortion to be corrected using MP model[1,3,11]. After this, the output is passed through an inverse modelling process, wherein coefficients are extracted for DPD signal generation to give output[3]. However, to overcome the drawback of direct implementation, phase unwrapping is applied before the multiplicative factor root $\sqrt[4]{\gamma_1(n)}$ (in the case of quadrupler, multiplicative factor=4), after which the output $\gamma_2(n)$ is then passed through the quadrupler to give $\gamma(n)$. The input-output relationships for above in pretext of Fig 2, can be defined by following Eqn.[1,3]:

$$\gamma_1(n) = \sum_{m_1=0}^{M_1-1}\sum_{m_2=0}^{M_2-1}\cdots\sum_{m_n=0}^{M_n-1}\sum_{k=1}^{K} c_{m_1 m_2 \ldots m_n k}\cdots$$
$$\ldots\beta(n-m_1)\beta(n-m_2)\ldots|\beta(n-m_n)|^{k-1} \tag{8}$$

Here, memory depth, nonlinear order & complex coefficients of the inverse model are defined by $M_1, M_2 \ldots M_n$, k and $c_{m_1 m_2 \ldots m_n k}$ respectively.

From previous Eqn. (8) $c_{m_1 m_2 \ldots m_n k}$ can be derived & subsequently then $\gamma_2(n)$ can be derived as follows[1,3]:

$$\gamma_2(n) = |\gamma_1(n)|^{\frac{1}{F}} e^{j\frac{\theta(n)}{F}} \tag{9}$$

The output $\gamma(n)$ can then be given as follows:

$$\gamma(n) = F.\gamma_2(n) \tag{10}$$

where, F is the multiplying factor of the frequency multiplier and F=4 for a quadrupler.

2.3 New Modified Polynomial Model Computational Approach (NM-PMCA)

This approach was initially proposed in the paper[1], wherein the input signal $\beta(n)$ is first pre-processed before being applied, i.e., at first, it is passed through 4th root to lead to $\sqrt[4]{\beta(n)} = \beta_1(n)$ as an output. Further, in this approach, $\beta_1(n)$ is phase unwrapped and gain unwrapped to give output as $\beta_2(n)$.

In the next phase, this is now passed through the DPD system model, whose output in offset and square formations is as in Eqn. 11[1]:

$$\gamma_1(n) = \sum_{k=0}^{M}\sum_{q=0}^{Q-1}\mu_{q,k}\beta_2(n-k^2)|\beta_2(n-k^2)|^q$$
$$+\sum_{k=0}^{M}\sum_{q=0}^{Q-1}\mu_{q,k}\beta_2(n+k^2)|\beta_2(n+k^2)|^q \tag{11}$$

In the above equation, q denotes the order and memory depth is denoted by k. Further, $\gamma_1(n)$ is then passed through a frequency quadrupler to give output $\gamma(n)$. The diagrammatic representation of this approach is represented in Fig. 3.

2.4 Proposed Computational Approach for Frequency Quadrupler

The results using the approach proposed in 2.3 can be further extended & optimized by using WT MS-PCA, i.e., wavelet MS-PCA. Thus, an in-depth analysis of PCA, wavelet decomposition and their implementation in frequency quadrupler is covered in this section.

2.4.1 Principal Component Analysis (PCA)

In literature[13,16], principal component analysis is used to reduce the dimensionality by identifying variance at the global level in the data set. i.e., matrix $P=[j_1,j_2,\ldots j_i]$ can be defined: first using eigenvalue decomposition for **A** observation matrix defined by **A**=L*(M+1)(N+1),$J=[j_1,j_2\ldots j_{(M+1)(N+1)}]$ as eigenvector. The main data point is that the projection of data is to low dimensionality space by new observation matrix **V**=**AP**, dimensions of new observation matrix **V** is reduced from L*(M+1)(N+1) to L*I[13,16], which means a reduction in coefficients as well from (M+1)(N+1) to I[16] & **y**=**VD**.

D=$[d_0,d_1..d_i]^T$, Ix1 vector[13,16] of PCA coeff. Thus, PCA is done using a correlation matrix and eigen value decomposition[13,16], wherein the new matrix is selected with principal components using eigenvalue weights of data variance, which can be implemented using classical polynomial models as well[13]. In order to not just focus on global variance as in PCA, local variance also needs to be accounted for, which can be achieved using wavelet-based MS-PCA to improve signal quality. WT-MSPCA steps have been depicted in algorithm number 1. Mathematical explanation & implementation(s) of the proposed idea have been shown in the next sections.

2.4.2 Wavelet Decomposition

It helps to analyze frequencies at varied resolutions[17]. Wavelet decomposition is defined as[17]:

$$\beta(t) = \sum_{\tau} \alpha_{d0}(\tau)\eta_{d0,\tau}(t) + \sum_{d}\sum_{\tau} \mu_{d\tau}(\tau)\theta_{d,\tau}(t) \tag{12}$$

Here,

$\eta_{d,\tau}(t) = 2^{\frac{d}{2}}\eta(2^d t - \tau)$; $\theta_{d,\tau}(t) = 2^{\frac{d}{2}}\theta(2^d t - \tau)$

d = dilation parameter, τ =translation parameter

$\eta(t)$ =scaling function, $\theta(t)$ =wavelet function,

α_{d0} :approximate coefficient; $\mu_{d\tau}$:detailed coefficient

For Wavelet decomposition, the following steps are covered:

2.4.2.1 Wavelet Function Selection

The primary step is selecting the wavelet (mother) based on data. The most common mother wavelets in literature are as follows:

Haar Wavelet[18]: Simplest wavelet with piecewise function, hence benefits detection of edges. However, transitions at the edges might add artefacts.

Daubechies Wavelets[19]: This is one of the wavelets which can be utilized for noise removal and compression & supports localization in time.

Symlets[20-21]: Symlets are useful when symmetry is important; properties of wavelet functions are similar. It is used in applications: gaussian noise removal; in remaining cases, it is identical to Daubechies results

Coiflet Wavelet[21]: These are mainly orthogonal in nature, having vanishing moments. Wavelet comprises scaling & wavelet functions.

Biorthogonal Wavelets[21]: This is used where the realization of both reconstruction and linear phase filters needs to be done together.

For our experiments covered in section 5, Daubechies Wavelets have been implemented owing to noise removal, which supported the experiments and the results, thereby helping to increase the NMSE values, one of the leading performance metrics, which is covered in section 3 of this paper.

2.4.2.2 Data Decomposition

After the main wavelet selection, decomposition is performed to have wavelet coefficients at varying resolutions to create levels for decomposition. Data decomposition is implemented using successive low pass-high pass filters combination[13,17] to produce coarse, high-resolution approximates, respectively[17]. Passing through LPF-HPF is achieved by multiple stages to improve the results. Typically, the stages vary from 2-3 depending on the data; however, three stages have been considered for the experiment covered in the 3rd section.

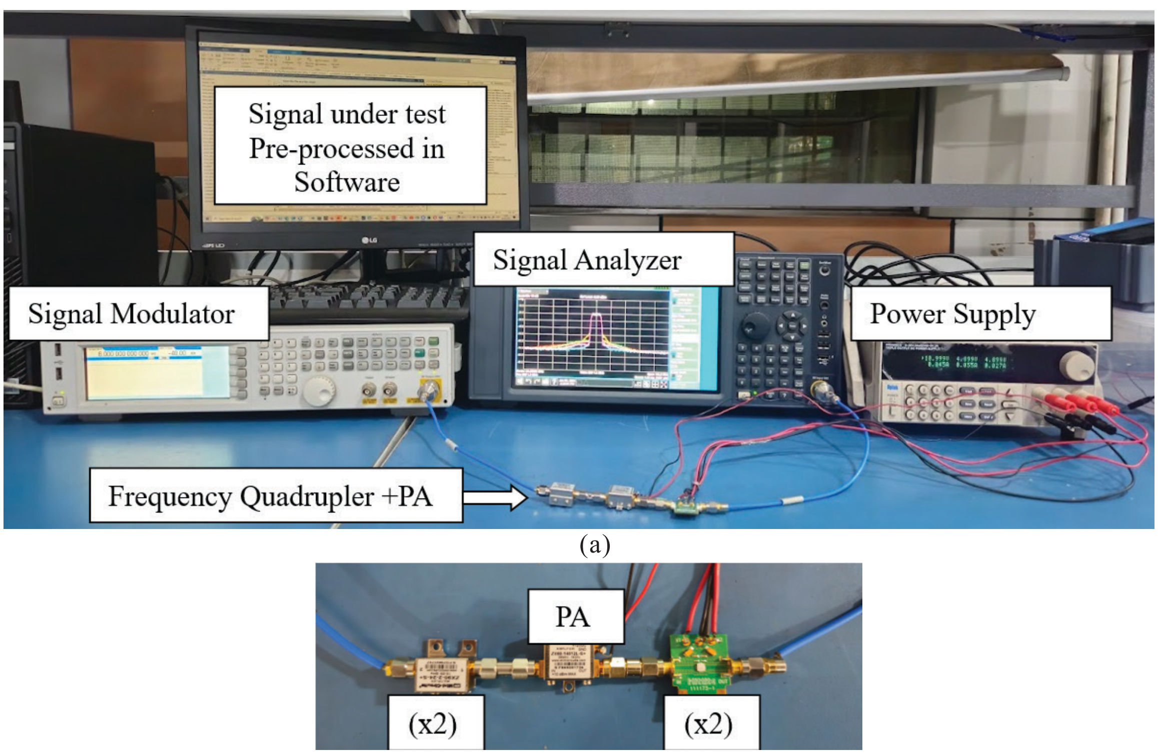

Figure 5. (a) Experimental test bench; and (b) Frequency quadrupler+PA used for experiment.

2.4.2.3 Thresholding

In the literature[17], the authors explained threshold detection by implementing hard/soft thresholding. The primary intent of thresholding, which is used in our implementation, is as follows:

Removal of noise: This step removes those coefficients that will not impact, i.e., mainly at noise level.

Dimensionality reduction: This step helps reduce the computations before the PCA step, which thereby helps reduce the complexity of computations. As in the algorithm 1 table post-WT-Decomposition, PCA is implemented, post which inverse WT is done, such that post the processing, coefficients so obtained passed for signal reconstruction which is the reverse process of signal decomposition wherein data is passed through LPF-HPFs [13].

Algorithm 1: WT-MSPCA methodology[13,17]
Step 1: Signal is passed through WT-Decomposition
Step 2: The output is then passed through the PCA
Step 3: Result goes through IWT for reconstruction of wavelet
Step 4: Reiterate with 3rd level WT- Decomposition
Step 5: Estimated output of the input is produced.

2.4.3 Implementation of Proposed Model in Frequency Quadrupler

The analysis discussed in sections 2.4.1 and 2.4.2 can be implemented as depicted in Fig. 4, wherein the input signal $\beta(n)$ was pre-processed and passed through the 4th root to give $\beta_1(n)$, which is then passed through phase and gain unwrap, its output $\beta_2(n)$ then passes through the system model which provides the output with: $\gamma_1(n)$ and post that it is passed through WT-MSPCA whose output is denoted by $\gamma_2(n)$, which was then passed to the last stage i.e, the frequency quadrupler, which can also be replaced by two frequency doublers whose output and as whole system's output is $\gamma(n)$.

3. EXPERIMENTAL IMPLEMENTATION & PERFORMANCE METRICS

3.1 Experimental Setup

To physically realize the theory proposition discussed in section 2, an experimental setup, as shown in Fig 5. was done. To set up a frequency quadrupler with the input of 6 GHz, two multipliers, ZX90-2-24-S+ and HMC 576L3B, with a range of 10 to 20 GHz and 18 to 29 GHz, respectively, were implemented. In addition, to overcome the attenuations at these frequencies, a power amplifier (ZX60-146012l-S+) with a range of 300 KHz to 14GHz was used with the first multiplier (ZX90-2-24-S+) and before the output of the second multiplier (HMC-576L3B). The test bench was also comprised of a vector signal generator (MXGN5182B) and vector signal analyzer (MXAM9020B) with a range capability of capturing output of 26.5 GHz, which was utilized for the experiment.

3.2 Signal Under Test

The signal used for the test was a baseband signal with a bandwidth of 10 MHz and a sampling rate of 184.32 MSPS. The signal is modulated at 6 GHz frequency using a vector signal generator (MXG).

3.3 Implementation of Experiment

Based on the experimental setup in section 3.1, mathematical analysis, which was done for the proposed computational approach with WT-MSPCA, other state-of-art approaches & new approaches discussed in section 2 were performed in MATLAB. Once it was done, the test signal was passed through it. The output of the mat file was then loaded into a vector signal generator, which then modulated the signal at 6 GHz. The modulated signal was then passed over the coaxial wire and passed via one frequency multiplier (ZX90-2-24-S+) post which the attenuated signal was boosted by a power amplifier (ZX60-146012L-S+). Then it was passed to a 2nd frequency multiplier (HMC576LC3B) to have an output frequency of a quadrupler of the order of ~24GHz. Once the quadrupler frequency is achieved, the signal is then passed to a vector signal analyzer (MXAN9020B) via coaxial wires, which were then subsequently analyzed based on performance metrics (discussed in section 3.4) and the power density spectrum curves and in-depth comparative analysis has been shown in results and discussions section of this paper.

3.4 Performance Metrics

Performance parameters in this section were utilized during experimentation to evaluate the proposed computational approach (covered in section 2.4). These parameters enabled the measurement of the results against the current literature methodologies, which helped provide a comparative analysis (covered in section 5). These performance metrics act as a benchmark to validate experiment results to the theoretical and mathematical approaches covered during the system-level discussion. In this paper, the following primary performance metrics have been covered for lucid validation of methodological approaches and their proofs of concepts.

3.4.1 Normalized Mean Square Error (NMSE)

NMSE is used to check the in-band errors. This benchmark helps to determine the performance of the system. By analyzing the NMSE, the signal quality can be compared and enhanced/optimized. NMSE can be defined as below:

$$NMSE = \left. \frac{\sum_{n=1}^{N} | y_d(n) - \widehat{y(n)} |^2}{\sum_{n=1}^{N} | y_d(n) |^2} \right|_{dB} \tag{13}$$

where, $\widehat{y(n)}, y_d(n)$ and N signifies estimated $y(n)$, desired value of $y(n)$ and length of waveform respectively. In the above equation, an in-band error can be expressed by δ which is equivalent to $| y_d(n) - \widehat{y(n)} |$

3.4.2 Adjacent Channel Power Ratio (ACPR)

This metric is used to measure performance by considering out-of-band errors. ACPR compares the power of an error-constrained signal in adjacent channels to the power of the main channel. This metric is also a very crucial parameter for maintaining signal quality.

Mathematically, the concept of ACPR can be defined as follows:

$$ACPR = \left. \frac{\int_{adj} |\chi(f)|^2 \, df}{\int_{ch} |\chi(f)|^2 \, df} \right|_{dB} \tag{14}$$

where,

$\int_{adj} |\chi(f)|^2 \, df$: Adjacent channel power

$\int_{ch} |\chi(f)|^2 \, df$: Desired channel power

4. RESULTS AND DISCUSSION

In order to validate the proposed methodology discussed in sub-section 2.4, extensive analysis and comparison were made based on metrics of performance as described in sub-section 3.4 with respect to the state-of-the-art approaches and new approaches in the literature using experimental setup (as shown in sections 3.1 through 3.3). The results based on the hardware experimental setup, in Fig. 5, have been discussed in the following subsections :

Table 1. Comparison of models in literature vs proposed model

Model	NMSE (dB)	ACPR (dB)
MP model + SCA[1,11,14]	-30.4	-38.5
GMP model + SCA[1,11,14]	-30.5	-40.3
NM-PMCA model[1]	-31.1	-48.3
MP model +WT-MSPCA [13,22]	-30.8	-41.8
GMP model + WT-MSPCA[13,22]	-31	-43.8
Proposed model [This work]	-31.5	-51.5

(MSPS=184.32, Bandwidth=10 MHz, NonLinearity Order=10, Memory Depth=4)

4.1 Hardware Experimental Results in terms of Power Spectral Density

Comparison results of power density spectrums of all waveform outputs coming in spectrum analyzer as shown in Fig. 5(a) coming from hardware setup are shown in Fig. 6. Since the input frequency was 6 GHz as discussed in section 3 of the experimental setup, the output centre frequency of all waveforms is 24GHz which is aligning to frequency quadrupler expectations. The spectrum analyzer outputs were overlapped for all models of interest, which were covered in mathematical and system models in section 2. The model outputs captured from the spectrum analyzer were: MP+SCA, GMP+SCA, NM-PMCA, MP+WT-MSPCA, GMP+WT-MSPCA, proposed model, gain-phase unwrapped signal and original LTE signal, which were measured in hardware described in sub-section 3.1.

The output waveforms prove the theoretical and mathematical foundations covered in section 2 in a methodological manner that the gain-phase unwarp, standard computational approaches help reduce the ACPR compared to the original LTE signal. Also, the graph shows that we see benefits in ACPR values going from state-of-the-art SCA approaches to NM-PMCA approach[1] to WT-MSPCA approach.

The result in Fig. 6, depicts that the ACPR of the proposed model decreases around 11.5 dB vs the GMP+SCA approach and decreases around 13.3 dB when compared to the MP+SCA approach. This result also extends the result of NM-PMCA[1] wherein the proposed approach presented in this paper shows the benefit of 3.2 dB as compared to the approach presented in the paper[1] with all other parameters such as nonlinearity order, MSPS, BW, and memory depth kept similar to each other.

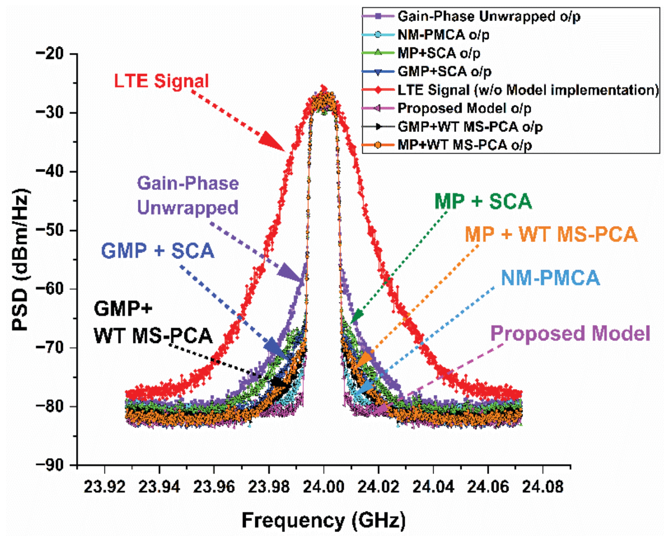

Figure 6. PSD comparison of proposed vs models in literature.

4.2 Comparative Study of Proposed vs Models in Literature

Based on the experimental setup shown in section 3, the results for both NMSE and ACPR are summarized in Table 1. The results show that for a given nonlinearity order of 10, memory depth of 4 and 184.32 MSPS signal. Per expectation and system-level discussions in section 2, a decrement of 1.8 dB in ACPR from the MP model +SCA to the GMP model+SCA is seen. Also, the ACPR decrement from the GMP model+SCA to the NM-PMCA model was seen to be 8 dB. In the next phase, it has been observed that WT-MSPCA models show a decrease of 3.2 dB to 3.5 dB in ACPR (whose theoretical modelling concept has been covered in section 2.4).

It is also observed that there is a decrement in 3.2 dB ACPR of the proposed model in this paper compared to the previous NM-PCA model[1]. This proves that WT-MSPCA helps decrease ACPR. Another valuable data point to be observed is that at the time when ACPR is decreasing, NMSE is not increasing or it is decrementing in the ballpark of 0.5 dB, i.e., without affecting NMSE/ with a slight improvement in NMSE, substantial improvement in terms of ACPR is observed using the above methodology, which is also observed in Fig 6. Regarding the power density spectrum and the comparative study of polynomial-based models of interest using standard computational approach(s), the NM-PMCA approach[1] and the proposed methodology proposed here have been documented in Table 1.

5. CONCLUSIONS

The current paper portrays the current trends in frequency multipliers and quadruplers. It delves deeper into the mathematical aspects of current relevant models in literature. It also extends the methodological model proposed in the paper[1] to a more computationally efficient version by introducing and analyzing the wavelet transform multiscale principal component analysis technique (WT-MSPCA). The paper first establishes the mathematical extension of the approach and then shows the results in actual using an experimental setup. The results are then compared with current models for ACPR using power spectrum density curves of all models. The improvement shows that the proposed approach helped improve 11.5 dB and 13.3 dB ACPR over GMP+SCA and MP+SCA models, respectively. The proposed model approach also shows around 3.2 dB improvement in ACPR value with respect to NM-PMCA[1], with all other constraints, namely bandwidth, nonlinearity order, sampling rate and memory depth as constant.

REFERENCES

1. Arora, D.; Tripathi, G. C. & Rawat, M. Frequency quadrupler based high-frequency vector signal generator using digital predistortion, 2024. *In* Proceedings of Second International Conference on Microwave, Antenna and Communication (MAC), Dehradun, India, 2024. doi:10.1109/MAC61551.2024.10837239
2. Park, Y.; Low, K.M. & Kenney, J.S. Digital predistortion linearization of frequency multipliers, *In* Proceedings of IEEE MTT-S International Microwave Symposium Digest, 2003. doi:10.1109/MWSYM.2003.1210465.
3. Liu, Y.; Liu, G. & Asbeck, P.M. High-order modulation transmission through frequency quadrupler using digital predistortion. *IEEE Transact. on Microwave Theory and Technol.,* 2016, **64**(6), 1896-1910. doi:10.1109/TMTT.2016.2561276
4. Clark, C.J.; Chrisikos, G.; Muha, M.S.; Moulthrop, A.A. & Silva, C.P. Time-domain envelope measurement technique with application to wideband power amplifier modeling. *IEEE Transat. on Microwave Theory and Techol.,* 1998, **46**(12), 2531-2540. doi:10.1109/22.739245
5. Kim, J. & Konstantinou, K. Digital predistortion of wideband signals based on power amplifier model with memory. *Electronic. Lett.*, 2001. doi:10.1049/el:20010940
6. Chani-Cahuana, J.; Landin, P.N.; Fager, C. & Eriksson, T. Iterative learning control for rf power amplifier linearization. *IEEE Transact. on Microwave Theory and Technol.*, 2016, **64**(9), 2778-2789. doi:10.1109/TMTT.2016.2588483
7. Schoukens, M.; Hammenecker, J. & Cooman, A. obtaining the preinverse of a power amplifier using iterative learning control. *IEEE Transact. on Microwave Theory and Technol.*, 2017, **65**(11), 4266-4273 doi:10.1109/TMTT.2017.2694822
8. Shipra; Tripathi, G.C. & Rawat, M. Power amplifier linearization in the presence of crosstalk and measurement noise in MIMO system. *IEEE Transa. on Circuits and Systems II: Express Briefs,* 2022, **69**(10), 3988-3992. doi:10.1109/TCSII.2022.3178616
9. Liu, Y; Liu, G. & Asbeck, P.M. Frequency quadrupling transmitter architecture with digital predistortion for high-order modulation signal transmission. *In* Proceedings of IEEE Radio and Wireless Symposium (RWS), 2015. doi:10.1109/RWS.2015.7129771
10. Cao, T.; Liu, Y.-J.; Jiang, J.; Zhang, Q.; Lin, C.; Yang, D.; Zhang, G.; Yang, C. & Zhou, J. Frequency multiplier-based millimeter-wave vector signal transmitter using digital predistortion with constrained feedback bandwidth, *IEEE Transact. on Microwave Theory and Technol.,* 2020, **68**(5), 1819-1829. doi:10.1109/TMTT.2019.2961085
11. Tripathi, G.C. & Rawat, M. High-frequency signal generator using cascaded frequency multiplier, *IEEE Access*, 2023, **11**, 74559-74568. doi:10.1109/ACCESS.2023.3295491
12. Morgan, D.R.; Ma, Z.; Kim, J.; Zierdt, M.G. & Pastalan, J., A generalized memory polynomial model for digital predistortion of rf power amplifiers. *IEEE Transact. on Signal Proce.*, 2006, **54**(10), 3852-3860 doi:10.1109/TSP.2006.879264
13. Tripathi, G.C. & Rawat, M. Analysing digital predistortion technique for computation-efficient power amplifier linearisation in the presence of measurement noise. *IET Sci., Measure & Technol.,* 2021, **15**, 398-410 doi: 10.1049/smt2.12041
14. Chung, A.; Darwish, A.M.; Viveiros, E.; Hung H.A.; Mitran, P. & Boumaiza, S. Analysis and compensation of nonidealities in frequency multiplier-based high-frequency vector signal generators. *IEEE Transact. on Microwave Theory and Technol.*, 2019, **67**(6), 2270-2283 doi:10.1109/TMTT.2019.2909901
15. Almoneer, M.; Mitran, P. & Boumaiza, S. Wideband digital predistortion for frequency multipliers driven by nonideal upconverters. *IEEE Microwave and Wireless Technol. Lett.,* 2023, **33**(1), 82-85. doi:10.1109/LMWC.2022.3200553
16. Jaraut, P. & Rawat, M. Application of principal component analysis based effective digital predistortion technique for low-cost FPGA implementation, *Int. J. RF and Microwave Comput.-Aided Engin.*, 2017, **27** doi: 10.1002/mmce.21095
17. Allabakash, S.; Yasodha, P.; Venkatramana Reddy, S, & Srinivasulu P. Wavelet transform-based methods for removal of ground clutter and denoising the radar wind profiler data. *IET Signal Process.*, 2015, **9**, 440-448. doi: 10.1049/iet-spr.2014.0312
18. Lepik, U. & Hein H. Haar Wavelets. Springer International Publishing, 2014. doi:10.1007/978-3-319-04295-4
19. Daubechies, I. Ten Lectures on Wavelets. *Soc. Industrial and Appl. Mathe.*, 1992. doi:10.1137/1.9781611970104
20. Wen, C. & Zhou, C. The feature extraction of rolling bearing fault based on wavelet packet-empirical mode decomposition and kurtosis rule, emerging technology for information systems. *Comput. Manage.*, 2013, **236,** 579-586. doi:10.1007/978-1-4614-7010-6_65
21. Akujuobi, C.M. Wavelets and wavelet transform systems

and their applications: A digital signal processing approach. Springer International Publishing, 2022, 13-44 doi:10.1007/978-3-030-87528-2_2

22. Tripathi, G.C. & Rawat, M. Robust linearization of power amplifier in the presence of transceiver noise *In* Proceedings of IEEE Asia-Pacific Microwave Conference, 2019, pp.1655-1657. doi:10.1109/APMC46564.2019.9038445

CONTRIBUTORS

Mr Devashish Arora obtained MTech degree in Electronics and Communication Engineering from IIT Roorkee. He is working at Qualcomm, India. His research interests include: Signal processing, software defined radios and image processing.
In the current study he shown proposed methodology and implemented it in the experimental setup.

Dr Girish Chandra Tripathi obtained PhD degree in Electronics and Communication Engineering from the IIT Roorkee. His research interests include: Analog and digital pre-distortion and software defined radios.
In the current study, he created the test bench/setup & apparatus, which was used for the experimental implementation of the results.

Dr Meenakshi Rawat obtained PhD degree from the University of Calgary and working as an Associate Professor at IIT Roorkee. Her research interests include: Software defined radio, digital and RF predistortion techniques.
In the current study, she provided guidance for the proposed modelling approach and experimentation of the given proposed model was done under her guidance.